Empirical evaluation of machine learning models for analysis of CoVID related diseases on different body organs

Supriya S. Thombre[1]*, Dr. Latesh Malik[2], Dr. Sanjay Kumar[3]

[1]*Research Scholar, Kalinga University, Raipur, Chhattisgarh, India.*

[1]*Assistant Professor, Yeshwantrao Chavan College of Engineering, Nagpur, Maharashtra, India.*

[2]*Associate Professor and HoD, Department of Computer Science and Engineering, Nagpur, Maharashtra, India.*

[3]*Department of Computer Science and Engineering, Kalinga University, Raipur, Chhattisgarh, India*

Abstract:

Corona Virus (or COVID19) has shown long-term effects on different human body organs, which include lung diseases, kidney malfunctions, heart dysrhythmia, changes in brain nutrient levels, psychological issues, abrupt changes in blood pressure, etc. Due to such a wide variation in the effects on different body parts, it is difficult for researchers to design models that can integrate these effects for treatment recommendations, and future disease prevention scenarios. Thus, this text reviews some of the recently proposed models that efficiently identify effects of COVID19 on different body organs. This review discusses the underlying models in terms of their clinical nuances, functional advantages, contextual limitations, and empirical future scopes. Based on this discussion, researchers will be able to identify optimal models for the identification of different diseases on individual body parts. It was observed that hybrid bio-inspired models, when combined with deep learning-based classification techniques, can efficiently identify these effects. This text also parametrically evaluates these models in terms of their accuracy, precision, classification delay, deployment cost, and scalability parameters, which will allow readers to identify optimal models for their performance specific use cases. To further contemplate this discussion, a novel COVID19 Classification Rank Metric (CCRM), which combines these parameters for comprehensive identification of optimal models is evaluated in this text. Based on this metric, researchers will be able to identify optimal models that can be deployed with high-accuracy, low delay, and high-scalability, along with lower cost for clinical scenarios.

Keywords: CoVID19, Body, Organs, Lung, Heart, Brain, Kidney, Classification, Disease, Bioinspired, Machine, Learning, Delay, Accuracy, Precision, Scalability, Cost, Scenarios

DOI Number: 10.14704/nq.2022.20.13.NQ88330 **Neuro Quantology 2022; 20(13):2627-2647**

1. Introduction

Originating in Wuhan, China, the C-19 (C-19) epidemic already infected individuals in large number throughout the globe. A rapid spread around the globe has ensured its success. Patients with SARS-CoV-2 who progress to clinical disease often have problems with their respiratory systems. However, the virus may cause damage to any organ in the human body. Those who are critically ill often have organ malfunction. [1] The virus will connect to vascular endothelial cells as well as cells in the heart, brain, kidneys, intestines, liver, and pharynx, and any other organs that carry ACE2 receptors. This might cause immediate damage to these organs. There is a risk that the virus-caused systemic disease may lead to organ malfunction. As part of their care, patients must have thorough physicals so that damage to internal organs may be assessed. Though coagulation and vascular endothelial abnormalities are fairly uncommon, they may first go unnoticed. There are several ways in which they contribute to organ dysfunction. Patients who eventually die away often have issues with both their heart and kidneys. Even when the acute illness has faded, there is a potential that the organs may continue to suffer damage. In the course of their lifetimes, organs face a wide range of possible impacts. Potential long-term damage exists. Rehabilitating a patient in a therapeutic environment may be time-consuming and difficult.

In addition to these, there may be oedema, endotheliosis, vasoconstriction, hypercoagulability, and inflammation. The patient has a low white blood cell count (low WBC), a high D-dimer, elevated fibrin degradation products (FDPs), lymphocytopenia, and disseminated intravascular coagulation (DIC). Instances of ischemic stroke, deep vein thrombosis, venous thromboembolism, pulmonary embolism, systemic arterial thrombosis and embolism, and myocardial infarction have been documented (MI). Myocarditis, arrhythmias, congestive heart failure, acute coronary syndrome, and other life-threatening heart conditions might result. Systemic disorders often cause damage to the kidneys. A stroke is a medical emergency that may happen to anybody at any age. Delirium and convulsions are common symptoms. Some people have reported having trouble with their sense of smell and/or taste. Both individuals and healthcare providers might have difficulties while dealing with mental health issues. It's possible that the by-products of waste contain a virus. Increases in lactate dehydrogenase could be possible. A widespread erythematous rash is only one of the many skin complaints that have been reported.

The SARS-CoV-2 virus may affect almost every system in the body by binding to ACE2 receptors, which are widely dispersed, are shown in various studies. A cytokine storm might ensue, leading to death. Various body-organs may be exaggerated by a variety of symptoms that are independent of both time and viral load. Inflammation, platelet activation, hypercoagulability, endothelial dysfunction, narrowed blood vessels, hypoxia, and muscle immobility are all contributing factors. The lungs are often affected. Myocarditis, heart failure, and acute coronary syndrome might all be happening at the same time to the patient. Patients should take their prescribed doses of angiotensin II receptor blockers and angiotensin, converting enzyme inhibitors. Systemic illnesses often caused AKI. Delirium, meningitis, encephalitis, and encephalopathy have all been linked to this outbreak. The sensations of smell and taste seem to have been compromised. Diseases often enter the body via the eyes because they are so easily penetrated. Both individuals and healthcare providers might have difficulties while dealing with mental health issues. The existence of gastrointestinal (GI) issues is supported by the available evidence. The skin condition is most often identified by the appearance of an erythematous rash in affected regions. Therefore, almost every internal organ may be vulnerable to the effects of C-19. As will become clear in the next section of this article, it is essential to conduct studies utilizing models that can assess the influence that C-19 has on the different organs of the body. Next, we'll do a quantitative empirical examination of the models under discussion, focusing on the values of the relevant parameters. It included some clinical data pertinent to those models and some ideas for approaches that might further enhance the functioning of the models that were evaluated in different situations in the last section of this research under different scenarios.

2. Literature Review

Researchers have proposed a wide range of clinical analysis models for identifying effects of C-19 on different body parts. A major portion of this research is done for estimation of C-19 effects on lungs, which is of the primary targets of virus receptors. In this section, a detailed analysis of different models is defined, and their performance levels for identification of different diseases are discussed in details. The models are clustered according to their effect on different body parts.

Models that cover multiple body regions

According to [1] there is a lack of information comparing the impact of the first and second waves of C-19 on Indian kidney transplant recipients. C-19 KTRs were collected in two waves, the first from March 15th, 2020 through December 31st, 2020 (n = 157) and the second from April 1st, 2021 through May 31st, 2021 (n = 102), with the results of the two waves being compared in a single retrospective analysis. The second cohort of KTRs consisted of younger persons (43 vs. 40; p=.04), whereas the first cohort had no podiatric patients (40 vs. 5.9%; p.003). It was shown that there were significantly fewer cases of cough (32 vs. 13.8 percent; p .001), secondary symptoms (45 vs. 62.7 percent; p .007), and fever (58 vs. 37.2 percent; p .001). The second group had lower levels of neutrophils (77 vs. 83%; p=.001), serum ferritin (439 vs. 688; p=.006), and lymphocytes (20 vs. 14%; p.001 for each). Tocilizumab (7% vs 0%, p.004) and hydroxychloroquine (11% vs 0%, p.0001) were more often prescribed during the first wave, whereas dexamethasone (27% vs 6%, p.0001) and remdesivir (47% vs 65%, p.03) were more commonly prescribed during the second wave. The incidence of mucor-mycosis (1.3 vs. 10%; p=.01) and admissions to the intensive care unit (20 vs. 37.2%; p.002) were also higher in the second wave. After 28 days, there was no difference in the death rate (9.6% vs 10%; p=1). No significant difference in mortality was seen between the two C-19 KTR waves at a leading transplant facility in India.

Patients infected with C-19 who could not fulfil inclusion criteria for randomized clinical research with remdesivir due to impaired renal or hepatic function were not allowed to participate. Hepatotoxicity and nephrotoxicity are two more side effects. After administering remdesivir to the C-19 103 subjects for 15 days, researchers evaluated their liver and kidney function. Just 20% of those seeking medical attention satisfied the inclusion criteria for randomized controlled trials. There was a drop in GFR [2] of at least 10 mL/min/1.73 m2 in 11% of individuals. The levels of aspartate and alanine transaminases went increased by 25% and 35%, respectively. Few cases of adverse health effects were reported. Based on these exploratory results, it seems that constant monitoring of renal and hepatic function may allow remdesivir administration in C-19 patients. They need to test their theory on a larger population of patients.

According to [3], SARS-CoV-2 causes the greatest harm to the kidneys and lungs. SARS-CoV-2 infection may worsen pre-existing renal impairment, making treatment more difficult and increasing the likelihood of patient fatality. The tubules of the kidney are damaged by SARS-CoV-2. Proteinuria is an important medical sign to watch for (PRT). Treatment for coronavirus should prioritize protecting the kidneys in order to reduce mortality (C-19). By analysing previous studies on renal illness and C-19 infection, this study aims to provide evidence-based recommendations for therapeutic anti-epidemic therapy.

Patients with both C-19 infection and renal failure had a higher mortality rate, according to research published in [4]. An increase in medicinal efficacy is possible if we can foresee death and KD. Hospitalized patients with C-19 in a multi-ethnic Asian nation will be the focus of an observational research that compares mortality and acute kidney injury (AKI) markers across several medical centres from January to June 2020. There were a total of 6078 participants in the trial. They were mostly Malay (71%), Chinese (6.7%), Indian (2.3%), and other (31.7%) males. Three point five percent of patients had acute renal damage, but only one point six percent had chronic kidney disease. (CKD). The yearly growth rate of GDP equivalents was 1.3%. Patients with AKI/CKD had a CFR of 20%. For several reasons, mortality and acute kidney injury were more common. After accounting for potential confounders, age (>70), Chinese ancestry, diabetes, and chronic renal disease remained as strong predictors of mortality as before. Predictors of AKI were diabetes, advanced age (>51), and initial presentation severity. The mortality toll among Chinese people was 2.58 times that among Malay people (p =.036). Artificial respiration and kidney dialysis were among the medical interventions needed to preserve a patient's life. Fever, coughing, and trouble breathing are the most common early indicators of AKI. Admission to the critical care unit, increased ventilation, and a longer length of stay are all related with low absolute lymphocyte counts. Acute kidney damage (AKI) and the severity of complications caused by the influenza virus (C-19) are affected by patient and environment factors. This research shows that this multi-ethnic Asian nation has significant gaps in mortality rates and access to medical care.

Research [5] indicates that SARS-CoV-2 is currently being treated as an outbreak. (C-19). Only around 5 percent of those who receive C-19 could get serious symptoms such organ failure, septic shock, or ADS. The kidneys are often impacted in some way. Kidney failure is characterized by acute renal damage and proteinuria (AKI). SARS-CoV-2 may directly infect podocytes and proximal tubular cells, which might have a number of consequences including acute tubular necrosis, protein leakage in Bradley's membrane, collapsed glomerulopathy, and mitochondrial dysfunction through an ACE2 route. Lymphopenia, macrophage activation syndrome, and cytokine storm are other potential contributors to AKI, in addition to SARS-CoV-2. Multiple causes, such as sepsis, rhabdomyolysis, hypercoagulability, interorgan interactions, and endothelial dysfunction, may lead to acute kidney injury. Hypoxia occurs when there is a lack of oxygen reaching the tissues, and this may cause kidney damage. Understanding the molecular etiology and pathophysiology of kidney damage and AKI in C-19 is critical for developing appropriate treatment protocols and medicines.

Professionals in the area recommend that researchers investigate the effects of hypoxemia on command-following recuperation times [6]. In this retrospective, multi-centre cohort study, researchers tallied the time it took for patients to regain control after intubation during the first wave of the US pandemic (March-July 2020). Cognitively impaired patients (motor score of 6 or below on the Glasgow Coma Scale) who needed endotracheal intubation for at least seven days were included. In 117 instances, patients regained the ability to comprehend and carry out instructions. For leadership to be restored after an emergency, allow 30 days (95% CI, 27-32). For patients with at least one episode of PaO2 55 mmHg, the median duration to regain command-following was 16 days (p 0.001), and 25% of patients recovered 10 days after breathing assistance. Persistent hypoxia reduced the chance of a command-following recovery (PaO2 70 HR = 0.88; PaO2 55 mmHg HR = 0.56; 95% CI = 0.46-0.68). These results were confirmed by a second surge group (N = 427, October 2020–April 2021) that did not include individuals with mild brain injuries (N = 199). Some weeks after stopping their supplemental oxygen, the C-19 survivors regain consciousness. After sitting for a while, hypoxemia becomes worse. Since this association cannot be explained by sedation or brain injury imaging data, it is advised that it should be taken into consideration when determining whether or not to continue life-sustaining treatment.

Experts in the medical field made the discovery in [7]. People with neurological illnesses in France were studied to determine their metabolic rates during the country's 55-day lockdown. Voxel-based positron emission tomography (PET) scans of the brains of 188 patients (mean age: 57.5 years 16.5; 114 males) showed a significant difference in the metabolism of 18F-FDG in the first 55 days after release from confinement compared to the same time period in 2019 before the SARS-CoV-2 pandemic (in 212 patients; mean age: 59.5 years 15.8; 114 men). Left amygdala, younger subjects, and the left dominant pyramidal tract were most affected, and recovery after 55 days of release was minimal. Furthermore, there was a negative relationship between solitary confinement and the metabolic rate of the sensory-motor brain. Hypo metabolism is associated with chronic obstructive pulmonary disease (COPD) patients, however the correlation is quite modest (9 percent). Physical inactivity, loss of fitness, and lack of social engagement have all been linked to disruptions in the brain's sensorimotor and affective processing networks. The kinetics of this metabolic pathway cannot be compared to COVID that has been artificially prolonged. Without more in-depth research into the long-term effects and linkages between cognitive and mental health and the functional deactivation theory, it would be irresponsible to extrapolate these findings to healthy confined individuals.

Medical experts in [8] report that millions of people have been affected by coronavirus disease 19 (C-19), a serious acute respiratory infection caused by coronavirus-2 (SARS-CoV-2). Some people infected with a serious illness may need extensive hospitalization and treatment. There may be a link between advanced C-19 and liver illness, since those with obesity and/or diabetes had a worse prognosis for the development of the virus. Due to immunological dysregulation and inflammation, people with CLD may be more susceptible to the symptoms of SARS-CoV-2. Early experiments using C-19 indicate that SARS-CoV-2 may cause direct liver damage in otherwise healthy infected individuals. COVIR-19 causes metabolic changes in the liver that may lead to CLD and mortality.

Research [9] suggests that the current coronavirus outbreak of 2019 (C-19) is caused by SARS-CoV-2. The leading causes of death from C-19 are acute respiratory distress syndrome and dispersed lung damage (ARDS). Acute respiratory distress syndrome may be predicted by the presence of C-19 hepatitis. Liver damage may result from SARS-CoV-2 infection in C-19 either directly or indirectly due to systemic inflammation, changes in hypoxia, iatrogenic factors including medication and ventilation, or worsening of pre-existing liver disease. The tropisms of SARS-hepatic CoV-2 and the acute and chronic liver damage produced by C-19 are discussed in this article.

Too far in 2019, millions of persons get infected with the new version of coronavirus viz SARS-CoV-2. Sixty percent or more of patients have loss of appetite, gastrointestinal distress, and vomiting. In addition, many people have liver biochemistry abnormalities. C-19-related liver damage is a distinct clinical issue (ILD). For starters, undiagnosed liver disease is a major health problem that gets short shrift. As a second point, several drugs now in widespread use may be harmful to the liver. There may be a number of variables that determine the extent of liver damage in critically unwell individuals. Researchers assess the current state of knowledge on the severity of liver injury in C-19 and provide diagnostic insights into key factors.

The 2019 Coronavirus Disease (C-19) pandemic has had serious repercussions for the treatment of acute cardiovascular issues [11]. Despite a failure in ACS hospitalized patients during the C-19, knowledge gaps remain about trends in, and treatment for, individuals with HF. People using ACEIs and ARBs may be at increased risk of contracting C-19. This research looked at how the C-19 crisis affected hospital mortality and HF admissions in Japan. Hospitalization records from Japan were evaluated to determine the extent to which C-19 is affecting patients with HF there. Our major metric of success was the weekly rate at which patients were admitted to the hospital because of HF. Hospitalization was necessary for 109 429 HF patients between April 2018 and July 2020. Three percent fewer HF episodes occurred each week after the emergency (95% CI, 0.3 percent to 6.7 percent; P = 0.03). When an emergency was declared, ACEIs and ARBs were administered at a rate of 4.2% (95% CI: 0.3% to 8.9%, P = 0.07). Mortality due to HF during hospitalization was not affected by the recent C-19 pandemic. In Japan, a decrease in hospitalizations of HF patients was seen, but there was not a correlation with the use of ACEIs or ARBs or an increase in in-hospital mortality.

[12] States that how C-19 affects the heart failure (HF) patients is still unknown. This study aims for determining how C-19 influences hospital mortality rates for HF patients. Patients hospitalized with HF who received a diagnosis between March 1, 2020 and May 6, 2020 were included in the research. C-19 was examined for its impact on mortality, kidney function, and heart damage in hospitalized patients. In the hospitalized HF group, 134 people contracted C-19. There was an increase in hospital mortality in COVI, cardiac injury, and acute renal damage. The findings of this research stress the importance of preventing C-19 infection in HF patients.

It has been suggested that the global C-19 epidemic has resulted in a shift in the way in which medical services are delivered to patients [13]. This research aims for determining how C-19 affects the mortality rate of AHF hospitalized patients. Poland's hospitals provided cardiac therapy to 101,433 patients between January 1 and December 31 of this year. In 2019, there were 9853 patients admitted to AHFs; in 2020, that number is expected to drop to 7546, a decline of 23.4%. (P 0.001). It has been shown that during the 2009 C-19 pandemic, self-referrals decreased by 27.8% (P 0.001) while ambulance transports rose by 15.9%. (P 0.001). Similar lengths of time were spent in the hospital. Deaths from AHF in hospitals increased from 444 (5.2%) in 2018 to 406 (6.5%) in 2020. (P 0.001). By 2020, 32% of AHF hospitalizations would additionally include patients with C-19. Hospitalized AHF patients with C-19 infection had a mortality rate between 31.4% and 44.1% between March 2020 and November 2020. They discovered that the C-19 pandemic increased ambulance transports for AHF patients, decreased hospital admissions for those with AHF, and increased hospital mortality rates for those with AHF; the fatality rate was highest for those who suffered from both AHF and C-19 at the same time.

In [14], researchers compared the risk factors of C-19 victim hospitalized due to any cardiovascular syndromes to HF disorder (Metabolic syndrome, abnormal lipid profiles, etc.). One of the goals of this research was to determine how common HF is and what effects it has on various patient subsets. A noteworthy effect was a decrease in deaths that occurred while patients were hospitalized. Twenty percent (or 122 people) of the C-19 hospitalized population in 1974 developed HF. 1282 of these patients (men make up 58% of the population, median age is 72, and the age range is 62 to 81) had cardiovascular disease or risk factors. Three hundred twenty-three (1282) out of the total number of hospitalized patients (325%) died. In-hospital mortality was greater among patients with HF (36%; n = 92) than among patients without HF. Still, HF was linked deaths (OR 1.45 [95% CI: 1.01-2.06], P = 0.041). One hundred eighty-six of 1282 (15%) hospitalized patients had an increased risk of dying while in the hospital because of acute HF (89 [48%] vs. 220 [23%]). (OR 3.10 [2.24–4.29], P 0.001). The mortality rate of hospitalized HF patients increases during the C-19 epidemic. Acute heart failure increases hospital mortality.

For the purpose of detecting and following C-19 from its asymptomatic beginnings to its eventual fatal end, the speech modelling (SM) and signal processing architecture presented in [15] is available. This approach sheds light on the complex interaction between the phonatory, articulatory, and respiratory aspects of human speech. This is because the upper respiratory tract—the larynx, pharynx, oral cavity, and nose—is immune to C-19 infection, whereas the lower respiratory tract—the bronchial, diaphragmatic, and lower tracheal—are not. There is also some suggestion that neurological symptoms could be triggered by the infection. An exploratory research was conducted utilizing audio interviews with five participants to determine the difference in Cohen's d effect sizes between pre-C-19 (before exposure) and post-C-19 (after positive diagnosis but considered asymptomatic). Acoustic waveform amplitude was utilized to evaluate breathing coordination, laryngeal motion (fundamental frequency and cepstral peak prominence), and articulatory motion coordination (formant centre frequencies). Though highly dependent on a small number of individuals, smaller group-level impact sizes suggest more straightforward subsystem cooperation. Recording settings, unequal data volumes, and variations in voice state from pre- to post-time need to be accounted for in larger, more precisely generated validation datasets.

Employing an IoMT system based on the ballistocardiograph (BCG) to check on the patient's heart and lungs from afar [16]. A BCG sensor, an edge node, and cloud services make up the system as a whole. Together, edge nodes and cloud services enhanced the stability and performance of computations. At the network's periphery, nodes perform signal processing functions such as assessing data quality, separating BCG and respiration signals, and recognizing peaks. Cloud computing is used for many things, including smart computing, record keeping, and HR virtualization. According to the stated procedure, we determined that the MAESDAE for pulse intervals in a group of 25 people was 9.682 ms, and that the MAESDAE for respiration intervals was 22431.1 ms. The study's controls consisted of 186 healthy adults and C-19 patients who had just been released from the hospital. C-19 patients' respiratory rhythm recovers before their heartbeat. Patients with C-19 should be aware of the possibility of cardiovascular illness. Care for C-19 patients after therapy may benefit from their usage of remote monitoring.

According to research in [17], a global pandemic of SARS-CoV-2 will be underway by the start of 2020. There have been more than three million fatalities and C-19 has been shown to negatively impact both mental and physical health. Minor instances of C-19 must be isolated for 14 days while symptoms are monitored in case the disease progresses. This study examines impact of C-19 on patients' cardiovascular, pulmonary, and psychological wellbeing using a number of different methods of patient monitoring. The study authors analysed the problems with current methods and offered a wearable telehealth solution for tracking physiological parameters such body temperature, pulse rate, blood oxygen level, respiratory rate, blood pressure, and cough. Artificial intelligence, sensor fusion, and machine learning might use this information to make predictions about lung function. The prototype gear and smartphone software produced promising results that were on par with or even superior than those of similar commercial offerings. The suggested technique may serve as a viable wearable alternative for the ongoing C-19 victims and victims of long-lasting illness who are under observations.

Acute cardiovascular disease (CVD), particularly ST segment elevation myocardial infarction (STEMI), [18] a major cause of death globally, requires rapid detection and treatment to reduce the high mortality and morbidity rates. During a pandemic like C-19, it is crucial to reduce the danger of cardiovascular crises and the chance of infection. This research proposes integrating wearable technology with mobile health (mHealth) apps for early identification and continuous monitoring to solve this problem. Infection risk among patients with acute CVD may be reduced if care providers follow these recommendations.

Twenty-five percent of C-19 patients admitted in ICU need external aeration, as per research [19]. There is still a need for the development of a reliable, objective technique of identifying whether patients with very modest diseases might gain anything from ventilator assistance. In this investigation, 869 individuals with a history of chest CT scans and similar clinical features were analysed (D1: 822, D2: 47). For dataset D1, N = 216 + 47 was utilized for testing, whereas for dataset D1, N = 606, or 70% of the dataset, was used for training. A specialized radiologist discovered GGOs and consolidation zones in the D 1 train compartment (N = 88). In order to identify whether or not a patient with C-19 will need mechanical ventilation, we used the D 1 data set to train an image artificial intelligence predictor (AIP). AIP's AUC for the D test was 0.81, making it independently predictive after correcting for potential confounding factors (p0.001). ClAIN outperformed AIP by an impressive 0.84 times on the D test (p = 0.04). ClAIN surpassed AIP in predicting patients who would need a ventilator for C-19. ClAIN may be able to detect C-19 patients who are severely unwell and need mechanical breathing, according to data from numerous sources.

According to [20], the C-19 virus has been linked to several instances and deaths around the globe. Early diagnosis, isolation, and treatment are crucial for effective pandemic responses. Researchers in this paper look into the issue and propose a blockchain-based solution that makes use of decentralized data storage, intermediates for re-encryption, and autonomous authentication. Their strategy ensures that all C-19 participants are issued DMPs and immunity certificates. Researchers have developed smart contracts on the Ethereum blockchain that will let healthcare providers give timely replies while protecting their patients' personal medical identities. Scientists have shown that DMP may shorten reaction times in healthcare institutions, restrict the transmission of incorrect information using immutable blockchain, and even halt the spread of illness. The researchers provide a thorough account of the process by which the suggested treatment was conceived, manufactured, and tested. The code uses on-chain events to make the method more practical for less costs.

Work in [21] asserts that proper lung lobe segmentation from CT scans is essential for the diagnosis of pulmonary illnesses. Particularly useful for recent attempts have been convolution neural networks. The convolution makes it impossible for them to accurately grasp structural connections. The veins, airways, and pleural wall are all affected by the boundaries and shapes of the pulmonary lobes. Finding the correct pulmonary lobes in C-19 or COPD patients requires careful consideration of anatomical connections, say researchers. Researchers provide a relational technique (RTSU-Net) that makes use of a non-local neural network module to capitalize on existing connections. The module formulates self-attention weights by taking into account geometric and visual connections between convolution features. Using just the C-19 training data, the researchers train and verify RTSU-Net on 5,000 patients with COPD Gene (4000 for training and 1000 for evaluation). Using information gleaned from the COPD Gene, researchers screened 470 C-19 patients using RTSU-Net (370 for retraining and 100 for evaluation). Than combat C-19 lung infection, RTSU-Net is superior to three other baselines.

The C-19 represents a serious threat to every nation as soon as it spreads world-wide [22]. Auto segmentation of lung infections from CT images is crucial for processing C-19 data. Uncompleted C-19 datasets are at the heart of the issue. Several lung lesion segmentation datasets that were not created for COVID may help address the C-19 segmentation challenge. Using a relation-driven collaborative learning technique with non-COVID lesions has been proposed as an efficient method for separating C-19 CT lung infections from their confounding non-infectious counterparts. The model makes use of a general encoder to keep track of lung lesion aspects unrelated to COVID, and a target encoder to keep track of properties relevant to the C-19 job. Researchers design a collaborative learning technique to enhance the model's generic and discriminative representation of C-19 infections by regularizing feature-level relation consistency. Several studies show that current performance may be improved by three percent in the Sorensen–Dice index and four percent in the normalized surface dice (NSD) if information from lesions outside of COVID is included. Their solution outperforms state-of-the-art segmentation techniques on big 2D datasets with CT slices. Their method has tremendous promise for application in the worldwide battle against C-19 since it can produce unique deep learning ideas with little annotation.

Lung ultrasonography (LUS), as stated in [23], is a low-cost, risk-free, and non-invasive imaging option. Inadequate numbers of skilled translators have slowed the spread of LUS. A paradigm for instructing deep neural networks in LUS comprehension has been devised to aid in its wider adoption. Using LUS to assess a patient's health requires careful consideration of sonographic artifacts like A- and B-lines and anatomical phenomena. Their technique involves adding anatomical data and LUS artifact channels to raw LUS frames. Traditional NN may be trained with the use of explicitly supplied domain knowledge for performing various tasks on LUS data. They combine the methods of using linear and convex probe LUS frames in their approach. For the purpose of assessing C-19's severity, ICLUS was used as a measuring stick. The C-19 severity predictions at the frame level were improved with the use of simple image classification algorithms. Using a semantic segmentation approach, the C-19 severity was determined for each individual pixel. Validating the efficacy of their strategy, their baseline models outperformed premium variants designed specifically for both goals.

Specialists in the medical field agree that early diagnosis of C-19 is critical for preventing a global pandemic and relieving burden on the healthcare structure [24]. Lung segmentation in CXR might help physicians spot lung illnesses in their earliest stages. There have been significant advancements in supervised lung segmentation recently, and deep learning is largely responsible for this. The lung area is not optimal for C-19 screening since it has seen domain shift and has little to no human pixel-level annotations. Multiple researchers have proposed a CXR lung area before multi-appearance C-19 screening framework. They proposes improvisation in cross-domain lung segmentation based model for multi-scale adversarial domain adaptation network in classification networks (MS-AdaNet). Lung region priors are then used to build a multi-appearance network (MA-Net) that can combine and extract features from many perspectives. MA-Net can provide predictions of common pneumonia, viral pneumonia, and C-19. MS-AdaNet is presently being evaluated using three different CXR datasets. AdaNet outperforms competing approaches in terms of MS-lung segmentation accuracy. In this case, MA-Net was used to filter out C-19, and the findings show that it worked well.

Autonomous C-19 diagnosis from CT scans was found to be limited due to a lack of labeled pictures, according to the study authors [25]. Researchers offer a label-free method for segmenting C-19 lesions on CT scans using voxel-level anomaly modelling, which recovers meaningful information from conventional CT lung imaging. The observation that at high intensities both arteries and tracheae exhibit distinctive patterns informed their models. Common CT lung pictures may have these patterns added to them by researchers utilizing voxel-level training and fake lesions. Researchers can tell the difference between healthy tissue and C-19 lesions by comparing and contrasting paired samples and then training a normalcy-recognizing network (NormNet). NormNet surpasses several other unsupervised anomaly detection (UAD) methods on three publicly accessible datasets. Models of isolated regions composed of a single body will be discussed in the next section.

Models that cover single body regions

Lung ultrasound (LUS) imaging may be useful for diagnosing lung diseases, as shown in [26]. Because of the ubiquitous nature of C-19, many individuals have had exposure to LUS data. Semi-quantitative classification of lung patients using a four-point rating scale. It has been suggested that the process of stratification might be automated with the use of deep learning (DL) algorithms that have been clinically validated. Data compression and automated decision-making in the context of pixel resolution and bit depth have not been studied. The purpose of this study is to assess DL on LUS data at a variety of pixel and Gray-level resolutions. We are testing the technique with 448 LUS recordings culled from 34 distinct patient evaluations. Quantization at 128-bit, 64-bit, and 32-bit, and resampling at 2x, 3x, and 4x all contribute to a final score for each video. The algorithmic score displays a little accuracy variation while evaluating intensity levels. Diagnostic agreement increased from 73.5% to 82.3% after intensity measurement and spatial down sampling. These findings indicate that 32-fold reduced data may be enough to offer prognostic agreement. allowing for efficient data processing even when limited means are at play.

The characteristics of ultrasonography as a radiation-free, portable, and repeatable technology make it ideal for detecting and evaluating C-19 Pneumonia (PN). Lung ultrasound scoring (LUSS) [27] was able to detect the increased lung fluid in C-19 PN with high sensitivity and specificity. Due to its high degree of subjectivity, LUSS must be evaluated by qualified medical professionals. Quantitative, automated lung ultrasonography grading was established for the assessment of the C-19 PN. In all, 31 C-19 PN patients with varying clinical presentations were included in the LUSS-based expert analysis of 1527 ultrasound pictures. The images were evaluated using a number of cutting-edge computer techniques, such as curve-to-linear transformation, pleural line recognition, region-of-interest (ROI) selection, and feature extraction. The LUSS was modelled based on the ROI's 28 characteristics. Using a 5-fold cross-validation, we evaluated LUS pictures using decision trees, support vector machines, and multilayer fully connected neural networks. To get an accuracy of 87%, a model of 128256 layers must be used on both the first and second layers. Clinical applications are possible for the described approach due to its ability to accurately and automatically assign LUSS to ultrasound pictures.

Some scientists are now studying DL-based techniques for detecting lung infections in the wake of the recent C-19 outbreak. Medical imaging is one area where deep learning (DL) has shown promise. This study employed DL to assess pictures for LUS, while the vast majority of previous research had relied on CT scans. A large database of LUS photos from several Italian hospitals has been compiled by the study's authors. Each image has been annotated at the frame, video, and pixel levels to show the severity of the underlying condition (segmentation masks). For completely automated LUS image analysis, these discoveries are utilized to train deep models. When it comes to pinpointing pathological artifacts and estimating illness severity, the deep network provided by the researchers—which was built using spatial transformer networks—fails miserably. Additionally, they provide a uni-norm-based approach for summing up frame scores throughout the duration of a film. The next step for the team is to look into deep models to determine biomarker segmentations in C-19 imaging. Successful experiments on the current dataset open the door to more research on DL for quicker C-19 identification using LUS data.

Recent research [29] suggests that people with C-19 may benefit from lung ultrasound (LUS) imaging. The assessment of LUS data is becoming more automated, and the resulting methods will be fair, efficient, and precise. This is backed up by the C-19 result. With the use of a hidden Markov model and the Viterbi algorithm, this work introduces an unsupervised approach to pleural line localization and recognition in LUS data. After the pleural line has been located, supervised classification using support vector machines is performed (SVM). Every LUS picture is run through a classifier to establish the patient's state of health or illness and, if the latter, the extent of the condition. The experimental verification of the technique's efficacy comes from linear and convex probe LUS data collected in Italian hospitals. When examining the pleura, linear probes are 94% accurate whereas convex probes only achieve an 84% success rate. When evaluating the severity of C-19-related pleural line anomalies, SVM classification provides an accuracy of 88%-94% when using convex probes and 94% when using linear probes. The gathered data, shown pleural line, and anticipated score chart allow for further investigation of the patient.

In 2019, according to [30], for initial detection and diagnosis of C-19, CT imaging data is essential. AI helped improve CT diagnostic' accuracy and usefulness. Evaluating CT images for C-19 pneumonia using existing supervised techniques requires laborious voxel-based annotations. In this research, an image-level labelling-based weak supervision technique for lesion localization in C-19 is created. First, CT slices from C-19 lesions were normalized using a GAN. In order to enhance the result, researchers used a specialized feature match approach which uses a good quality CT images. Lastly, the location of the lesion can calculated as the difference between the output images and its corresponding input image. The more accurate diagnostic tool was designed by adding the classifier to the GAN-based localization map. This study compares the CT statistics for C-19 from China Medical University, Italy, and Sao Paulo. The suggested approach is compared to fully supervised learning techniques for segmenting lesions in the C-19 database. In spite of this, a result with a Sorensen–Dice index of 0.575 may be produced with little oversight. Researchers found that the majority of those in the group with the most frequent severity also had the highest visual ratings, indicating that their technique may helped in the initial detection of C-19. The researchers also investigated whether or not there was a connection between the visual score and the degree of illness. The study's authors conjecture in their conclusion that this unique approach will lessen the load of high expenses connected to expert annotation, hence enhancing the precision of machine diagnosis for C-19.

Data from [31] suggest that C-19 is rapidly expanding its global footprint. Automatic lung infection segmentation from CT scans provides a fast and efficient way for C-19 detection and its medication which is especially important given the scarcity of clinicians and other resources. When comparing CT slices from different groups, you'll see a wide range of variation. The segmentation of lung infections is introduced using an adaptive neural network (AdNN). Both the autofocus and the panoramic modules gather semantic data, together with fine-grained features and interconnected context links. Additionally, the calibration procedure has access to a specialized structural consistency correction made possible by the contrasted foreground and backdrop. All of their work is double- and triple-checked by multi- and single-class C-19 CT scans. Their strategy is effective, as shown by the high mIoUs (64.8%, 65.2%, and 73.8%) they achieved on three C-19 benchmark datasets.

Despite the fact that lung ultrasound (LUS) scans with precise patterns are applied to determine the severeness of C-19 pneumonia, doctors' interpretations of these pictures are typically qualitative and subjective. In order to quantify the prevalence of C-19 pneumonia in LUS images, we do statistical analysis on pleural lines (PLs) and B-lines (BLs). There are a total of 13 individuals with mild pneumonia, 7 with intermediate pneumonia, and 7 with severe pneumonia who have contracted C-19. LUS images have their PL thickness (TPL), roughness (RPL), mean (MPLI), and standard deviation (SD) removed (SDPLI). The total number of BLs, average width, attenuation coefficient, and overall intensity are all included in the information that was returned. The severity of a disease may be affected by several factors. The data is split into severe and non-severe categories using different feature combinations, and each feature and Support Vector Machine (SVM) [32] classifier is then assessed on this dataset. There are four measures of lethality that relate disease severity to their respective terms: case fatality rate (CFR), number needed to kill (NBL), age at death (AWBL), and age at infection (AIBL (p0.05). When using all of the data points at hand, the SVM classifier performs the best (ROC = 0.96, sensitivity = 0.93, specificity = 1). The study's findings corroborate the idea that the suggested approach might be utilized to automatically assess the effectiveness of the diagnosis and subsequent therapy of C-19 pneumonia.

Millions of people in over 200 countries have allegedly fallen victim to the 2019 coronavirus illness (C-19) epidemic. Finding sick people and keeping them apart is crucial for stopping the spread of disease. The diagnostic value of RT-PCR cannot be overstated. Although RT-PCRs have a high degree of sensitivity, it is not high enough to successfully avert a worldwide epidemic. A chest CT scan has the potential to be very sensitive for early patient identification, complementing RT-PCR. It takes an average of 21.5 minutes to complete a chest CT scan. In this research, we provide a unique Joint Classification and Segmentation (JCS) approach for instantaneous diagnosis of C-19 chest CT. The researchers require 144,167 chest CT images from 350 controls and 400 C-19 patients to train the JCS algorithm. A total of 3,855 chest CT scans from 200 individuals are analysed for pulmonary opacities down to the pixel level. Annotations such as the number of lesions, the size of the opacification zones, and the placements of the lesions assist in the diagnosis. Analysis shows that the proposed JCS diagnostic approach successfully recognizes and segments C-19. Their COVID-CS classification test set Dice score is 78.5, sensitivity is 95.0, and specificity is 93.1.

Professionals in the medical field have said [34] that correct C-19 patient identification is crucial for prompt quarantine, treatment, and pandemic containment. The researchers introduces Multi-task Multi-Slice DL model for CT-based Multi-class Lung Pneumonia Screening, developed using training data and other available resources in mind (such as Time and Money). A pair of separate 2D convolutional neural network (CNN) models are used, one to categorize slices and the other to categorize patients. In contrast to the former, which aggregates and fine-tunes features from a large number of CT slices rather than small CT volumes for feature representations, the latter may be able to collect temporal information for pneumonia screening by aggregating slices. Their M3 Lung-Sys can discriminate between C-19 patients and healthy, H1N1, and CAP patients and can identify lesions without pixel-level annotation. Researchers put their strategy to the test on a dataset consisting of 734 chest CT scans. Their suggested method achieves better quantitative results than the status quo for both patient-level and slice-level categorization. The lesion location maps generated by their method improved readability for clinicians.

C-19-based disease types afflicted diabetics more severely than the general population due of their propensity for hyperglycemia, as previously shown. These days, most hospitals and clinics either use a central database or rely on patients to keep their own paper records. During a pandemic, it would be crucial to have access to and exchange data from the primary system. As part of this endeavour, a blockchain-based community [35] for persons with diabetes is built. If all parties in the healthcare system have access to information on diabetic patients, they may be able to prioritize oxygen beds, immunizations, compensation, telemedicine, 5G-integrated remote location help, and other services during a pandemic. An Ethereum sandbox might provide a secure place to save medical records for diabetes patients. In order to protect patient privacy, IPFS encryption is applied to medical records before they are stored on the blockchain. A blockchain proof-of-concept is currently being developed by this collaboration. It's denoted by the NEM symbol. Each consortium member is provided with a QR code created by NEM that may be scanned to get access to the information stored in the distributed database. Diabetes smart contract on the blockchain. Users are validated by ABE and malicious nodes are disabled. Based on these findings, it seems that merging many blockchain blocks into one bigger one might improve transaction speeds, lower costs, and minimize energy use.

The gene expression outlined dataset of mouse liver and spleen with tested mouse hepatitis virus is passed on to the Tensor decomposition (TD)-based unsupervised feature extraction (FE) [36]. It is possible that the genes hold clues on how coronaviruses propagate. Compounds were chosen from a public database and utilized to inhibit 134 genes in this investigation. In addition to virtual testing for their efficacy against C-19, several of the newly found medicinal compounds have been linked to other antiviral medications.

Artificial intelligence (AI) for the interpretation of chest X-ray (CXR) images for diagnosis and patient triage is crucial in light of the nationwide expansion of the C-19 epidemic. Since C-19 is an emerging pathogen, it is more difficult to get CXR data for DL networks. For the purpose of diagnosing C-19, it has been suggested to use a patch-based convolutional NN with few trainable parameters. Their statistical examination of CXR biomarkers [37] informed their suggested method. The saliency maps (CXR SM) generated by their technology have the potential to be employed in clinical practice for the diagnosis and classification of C-19 patients.

Scientists have discovered a new respiratory virus they are calling "Coronavirus Disease 2019" (C-19) [38]. It is crucial to understand or anticipate the trajectory of the C-19 outbreak, given the rapidity with which it spread and the diversity of experiences its victims have told. Most research on the spread of C-19 has relied on either outdated epidemiological models or unproven machine learning methods. With the goal of predicting the spread of C-19, this research introduces T-SIRGAN, a system that combines deep learning methods with epidemiological theory. The Susceptible-Infectious-Recovered (SIR) model generates data for epidemic simulation, which is subsequently fed into a GAN as adversarial examples for data augmentation using T-SIRGAN. Using the simulated data, Transformers makes predictions about C-19's behaviour. Extensive testing using real-world datasets has shown the efficacy of their method. A vaccination against C-19 is also being tested for its efficacy.

It has been suggested in the literature [39] that chest CT may help diagnose a coronavirus infection. (C-19). It is crucial to classify these instances using CT scans since medical experts from all over the globe are reporting more C-19 cases. Researchers recommend the AFS-DF categorization for C-19 based on data from chest CT scans. Extraction of key information from a CT scan is the first step in analysis. A deep forest model is used to learn a high-level representation of these qualities with little information. The C-19 classification model may be adaptively combined with the researchers' feature selection strategy to remove superfluous characteristics. In this method, the trained deep forest model is the backbone. The AFS-DF was used to assess 1495 C-19 patients and 1027 CAP patients (CAP). Their respective accuracies, sensitivities, specificities, AUCs, and F1-scores were 91.79, 89.59, 96.355, and 93.17%. According on experimental data, the suggested AFS-DF outperforms four popular machine learning algorithms in categorizing C-19 vs. CAP.

There is speculation that SARS-CoV-2 has sparked a worldwide epidemic [40]. As the RT-PCR-based SARS-CoV-2 testing regime has a reduced positive detection rate during the initial periods of C-19, it is unable to meet the current testing standards. Regular and comprehensive testing for C-19 calls for a new approach. Some of the answers might perhaps be found in deep neural networks and wearable medical sensors. By nature of their design, WMSs can keep tabs on critical indicators in real time and broadcast the results to the public. Unfortunately, despite progress, deploying WMSs/DNNs on edge devices with constrained resources remains challenging. CovidDeep (CDeep) combines robust DNNs with easily available WMSs to provide quick detection of infectious diseases under all conditions. When utilizing CovidDeep, feature extraction is not required. It may be completed on a mobile device, uses information from a WMS, and consists of straightforward questions. In all, 87 participants (both symptomatic and asymptomatic) were analyzed. The accuracy of trained DNNs for three-way classification was evaluated by testing them on subsets of data drawn from six WMS and questionnaire categories. With 98.1% success, this project was a resounding success. The models were shown to have high accuracy and low rates of false positives, false negatives, and F1 scores. The DNN architecture and weights were trained via a grow-and-prune synthesis technique, and a prior was added to the weights using a synthetic training dataset generated from the same probability distribution. Consequently, DNN required less space for storage and fewer floating-point calculations. It follows that Covid Deep DNNs are trustworthy and have low needs for data storage and processing power. High levels of patient privacy are maintained in mobile DNN apps. We will go on to discuss models for specific applications now.

Case-specific models

The biomedical research community may benefit from looking forward to possible shifts in the future [41]. The article uses the eigenvalue decomposition of the Hankel matrix (EDVHM) and the autoregressive integrated moving average to forecast nonstationary time series (ARIMA). Nonstationary in time series is defined inside the PowerPoint presentation. Time series that are not stationary may be analysed and dissected more easily with the help of EVDHM. To estimate the values of the components, we use an ARIMA-based model. Taking the sum of the projections for its constituent parts yields the whole system's expected value. Genetic algorithms (GA) are used to improve the ARIMA parameters for each subcomponent (AIC). To test the model's accuracy, the data on the expected amount of newly affected C-19 cases each day in Brazil, India, and the United States is used. The findings provide staggering proof of the method's success.

Quarantining and treating those who have been diagnosed with C-19 promptly is essential for a successful outcome, as stated in [42]. It also states the fully-automated, DL-based diagnostic model for chest CT scans. It is feasible to localize SARS-CoV-2, C-19, and lesions in 3D CT volumes using a weakly-supervised deep learning architecture. Initially, the lung area of each patient was segmented using a pre-trained UNet. Once the 3D lung area was segmented, it was added to a 3D deep neural network that could predict the infectiousness of C-19. As a conclusion, C-19 injuries were identified by combining the classification network's activation zones with the unsupervised linked components. For training, we employed a total of 499 CT volumes, whereas 131 were used for testing. Both the ROC and the AUC for their plan in terms of public relations were 0.959. Combining the method with a 0.5 probability threshold led to an accuracy of 0.901, a positive predictive value of 0.840, and a negative predictive value of 0.982 in identifying COVID-positive and COVID-negative events. A custom GPU took 1.93 seconds to process each patient's CT volume. A weakly-supervised DL network was built to recognize lesion locations in CXR and estimate the possibility of a C-19 infection without requiring lesion identification during training. High-performance deep learning technology may quickly identify C-19 patients, allowing for a cure for SARS-CoV-2.

SARS-CoV-2 is blamed for the 2019 Epidemic (C-19), according to [43]. (SARS-CoV-2). Pandemic and epidemic management relies heavily on serology testing and rapid, comprehensive molecular diagnostics. Researchers examine clinical data from the whole C-19 care continuum, from prevention to treatment to follow-up (i.e., in prevention, preparedness, response, and recovery). Scientific support for precise illness diagnosis is provided by studying viral RNA, antigens, and antibodies during human infection. Concerns for high-volume screening were investigated in this study. A consideration of clinical requirements may help in identifying areas where there are gaps in testing technology. Possible methods include modified polymerases, isothermal amplification, and direct amplification from complex matrices, while more recent developments like as CRISPR diagnostics, visual end point detection, and PCR-free nucleic acid sensing show promise for application in at-home testing. The world's public health infrastructure might be strengthened and future epidemics could be avoided with the aid of lessons gained and suggestions presented at C-19.

Clinical researchers made this claim in [44]. High-Risk Coronavirus Type 2 Illness (C-19) related to SARS (SARS-CoV-2). The higher death rate was observed in diabetic patients, patients with cardiovascular disorder and cancer. It was also observed in elder persons. Human proteins ACE2, TMPRSS2, and BSG interact with SARS-CoV-2 proteins. These three proteins formed the foundation of a protein-protein interaction sub-network that symbolizes viral invasion. Insulin resistance, AGE-RAGE signalling in diabetic complications, and adipocytokine signalling were all linked to diabetes, cancer, and cardiovascular disease. C-19's deadly effects may be traced back to the underlying biology of aging and its associated pathologies. Gene expression analysis has led to the identification of drugs that interfere with certain protein-processing pathways. Medications that have the potential to drastically lower ACE2 and associated protein levels were the primary focus of the research. When mocetinostat and entinostat were being tested for non-small cell lung cancer, COL-3 was shown to be useful in treating acute lung damage and respiratory distress. It has been suggested that these medications be modified to make them effective against C-19.

In view of the current epidemic and the resulting lack of medical resources, doctors have proposed deep learning algorithms for automated C-19 finding based on 3D CT scans [45]. However, present approaches do not account for the correlation between segmenting lesions in 3D and assigning diseases to those lesions. DeepSC-COVID is the first collaborative DL model for segmenting and classifying C-19 lesion data. Researchers used a large CT dataset consisting of 1,805 3D CT scans having fine-grained injury descriptions to find four discrepancies between C-19 and CAP (CAP). During the learning process, together with a task-aware loss, how 3D lesion and classification subnets may interact was shown. For determining the precise 3D location of all lesions, their C-19 model may be used. Extensive experimental data suggests that their approach enhances the accuracy and efficacy of 3D lesion segmentation and illness classification thanks to the joint learning architecture it employs.

Evidence from [46] suggests that the global spread of C-19 is damaging health service throughout the globe and endangering the lives of countless individuals. Lack of accurate diagnostic tools is the primary roadblock to effective treatment. In order to increase clinical accuracy and efficiency, chest X-rays may be automatically analysed for C-19 occurrences using deep learning-based AI. It is challenging to annotate chest X-rays on a large scale due to a lack of resources and the strain imposed on the healthcare system. Using just chest X-ray pictures, the MHA-CoroCapsule capsule network (CC Net) model with multi-head attention routing is developed to identify cases of C-19. In addition to convolutional layers, two capsule layers, and a parameterized multi-head attention routing strategy, the MHA-CoroCapsule also makes use of a non-iterative, multi-head attention routing method. The research uses a dataset that includes both C-19 pictures and non-COPD-related pneumonia photos. Even with a small sample size, the model maintains a high degree of accuracy, recall, and precision of 97% or higher. Comparatively, deep feature extraction and transfer learning need more trainable parameters than the suggested MHA-CoroCapsule.

Over 1.9 million people have perished throughout the world since the first verified case was announced in December 2019 and the new coronavirus pandemic was detected. CT scans are helpful for further diagnosis and therapy since lesions produced by COIVD-19 are easily seen on these images. Deep learning might be utilized to segment CT images of C-19-related lesions. Using patient's CT pictures infected with C-19, the authors of this research present a multi-point supervision network (MPS-Net) [47] for detecting lung lesions. Multi-scale input, multi-scale sieve connections, and multi-scale feature extraction are only a few of the supervised learning architectures included in the MPS-Net. In order to extract feature maps of varying sizes, both the sieve connection and multi-scale feature extraction structure use receptive fields of varying widths. A multi-scale input structure may reduce the amount of information lost in the convolution's borders. To accommodate the arrival of supervision signals from a number of up-sampling nodes in a network, the authors provide a multi-point supervision training architecture. In terms of diagnostic and operational utility, their model has a DSC of 0.8325, a sensitivity of 0.8406, a specificity of 0.9988, and an IOU of 0.742. The effects of the proposed network successfully segments C-19 in CT images, which will assist in the diagnosis of cardiac pneumonia and its subsequent treatment.

Too far, around 1,436,000 persons in over 200 countries and territories have been diagnosed with coronavirus infection (C-19) [48], according to estimates from clinical experts as of April 9, 2020. An immediate diagnosis is needed for C-19 therapy and management. The aim is to train a dual-sampling attention network for distinguishing between CAP and C-19 on chest CT images (CT). The authors recommend combining a 3D CNN having a web-based attention module to pinpoint the specific site of lung infections. From the onset of symptoms, C-19 seems to spread at varying speeds amongst regions. Researchers use a method called "dual-sampling" to mitigate individual disparities in learning. They have used C-19 data from 8 different universities to evaluate their approach. The training-validation process involves analysing a total of 2186 images derived from CT scans of 1588 individuals. Twenty-five hundred and seven CT images from 2,796 people are included in the analysis. If the suggested approach is utilized early in the pandemic, radiologists may be able to differentiate C-19 from CAP.

According to the [49] research, new C-19 suspicions need precise and prompt screening to allow for rapid quarantine and medical care. Deep transfer learning-generated CXR screening models could help detect and prevent C-19. The geographic complexity of CXRs makes C-19 screening difficult. The aim is to provide a DCov-Net-based transfer learning model for detecting possible C-19 carriers in CXR pictures. Network parameters are optimized via multi-objective simulated annealing (DCov-hyper-parameters MMCGA). Most of the C-19 diagnostic models are closed and hence difficult to use. Heat maps are a useful data visualization tool since they help to quickly identify patterns and trends. To operate, the MMCGA-based DCov-Net calls on four separate groups of data. The MMCGA-based DCov-Net beats its rivals was demonstrated in the experimental results. DCov-Net, built on top of MMCGA, offers a 99.34% sensitivity and a 0.51% specificity for detecting C-19 suspects.

As reported in [50], the C-19 pandemic has already started in 2019. Chest CT scans, C-19 patients shows lung damage evidence including ground-glass opacities (GGOs) and consolidation. The process of manually annotating anomalies for graveness analysis is laborious and lengthy. Therefore, we developed a visual technique for separating the lungs. For GGO and consolidation separation, the LwMLA-NET deep learning system was suggested. The LwMLA-NET uses depth-wise separable convolutions at every layer to reduce computing costs. Multilevel attention (MLA) allows for quicker optimization by focusing on the most important aspects while disregarding the less important ones. As the bottleneck is integrated with ASPP, scalability issues are reduced. With MedSeg, LwMLA-NET achieved an accuracy of 76.7%, while with Radiopedia, it achieved an accuracy of 73.1%. With respect to generalization and segmentation performance techniques, LwMLA-NET outperforms Attention U-Net, PSP-Net, Cople-Net, Inf-Net, and Mobile-Net V2 based systems. As a result, it is clear that there is a wide range of effectiveness, scalability, and application among the available models. The next section compares the models based on their real-time performance indicators under clinical situations, making model selection even easier for real-time use cases.

3. Statistical analysis of various COVID19 analysis models

From the detailed review of existing C-19 analysis models, it can be detected that these models are extremely variant in terms of their applicability and performance levels. Thus, in this section these models are compared w.r.t. their statistical metrics including accuracy (A), precision (P), classification delay (D), deployment cost (DC), and scalability (S) parameters. As most of these models showcase high variance in accuracy & precision performance under different conditions, thus these metrics along with others are quantized into fuzzy ranges of Low, Medium, High, and Very High, which will allow readers to compare these models on similar quantization levels. Based on this strategy, the comparison can be observed from table 1 as follows,

Model	A	P	D	DC	S
KTR [1]	Medium	Low	High	High	Low
GFR [2]	Low	Low	High	Very High	Low
PRT [3]	Medium	Medium	Very High	High	Low
AKI [4]	Medium	Low	High	Very High	Low
ACE2 [5]	Low	Low	Very High	High	Low
FDG 18F [7]	High	Medium	High	Very High	Low
CLD [8]	Medium	Low	High	High	Low
ARDS [9]	Medium	Low	Very High	High	Medium

ILD [10]	Low	Medium	Very High	High	Low
ACEI [11]	High	Low	Very High	Very High	Low
HF [12]	Medium	Low	High	High	Medium
AHF [13]	Medium	Low	High	Very High	Medium
PCHF COVI CAV [14]	High	Medium	Very High	Very High	High
SM [15]	Medium	Low	Medium	High	Medium
BCG MAE SDAE [16]	High	High	High	High	High
AI [17]	High	High	High	M	High
IoT STE MI [18]	High	Medium	High	Very High	Medium
ClAIN [19]	Medium	Low	Medium	Low	High
DMP [20]	High	Medium	Very High	High	High
RTSU Net [21]	High	High	Medium	High	High
CT Seg [22]	High	Medium	High	Medium	High
ICLUS [23]	High	Medium	High	High	High
MS Ada Net [24]	Medium	High	Medium	Low	Medium
Norm Net [25]	Very High	High	High	Medium	High
DL LUS [26]	High	High	High	Medium	Low
LUSS [27]	High	High	Very High	High	Low

ML LUS [28]	High	Medium	Very High	High	Low
SVM LUS [29]	Medium	Low	Very High	High	Low
GAN [30]	Very High	Very High	High	Medium	Very High
AdNN [31]	Very High	High	Low	Medium	High
eSVM LUS [32]	Medium	Low	High	High	High
JCS [33]	High	Medium	High	High	Low
M3 Lung Sys [34]	High	High	High	High	High
TDS FE [36]	Medium	High	High	High	High
CXR SM [37]	Medium	Medium	High	Very High	High
TSIR GAN [38]	Very High	High	High	Medium	Very High
AFS DF [39]	High	High	High	High	High
CDeep [40]	Very High	Very High	Low	Medium	Very High
ED VHM [41]	High	High	High	High	High
UNet [42]	Very High	Very High	Medium	High	Very High
CRI SPR [43]	High	High	High	Very High	Low
AGE RAGE [44]	High	High	High	High	Low
Deep SC [45]	Very High	High	Medium	Very High	High
CC Net [46]	High	Very High	Medium	Low	Very High

MPS Net [47]	Very High	High	Very High	High	High
3D CNN [48]	Very High	Very High	High	Medium	High
DCov Net [49]	Very High	High	Very High	High	High
Lw MLA Net [50]	Medium	Very High	Very High	High	High

Table 1. Empirical evaluation of different models for identification of CoVID19 side effects

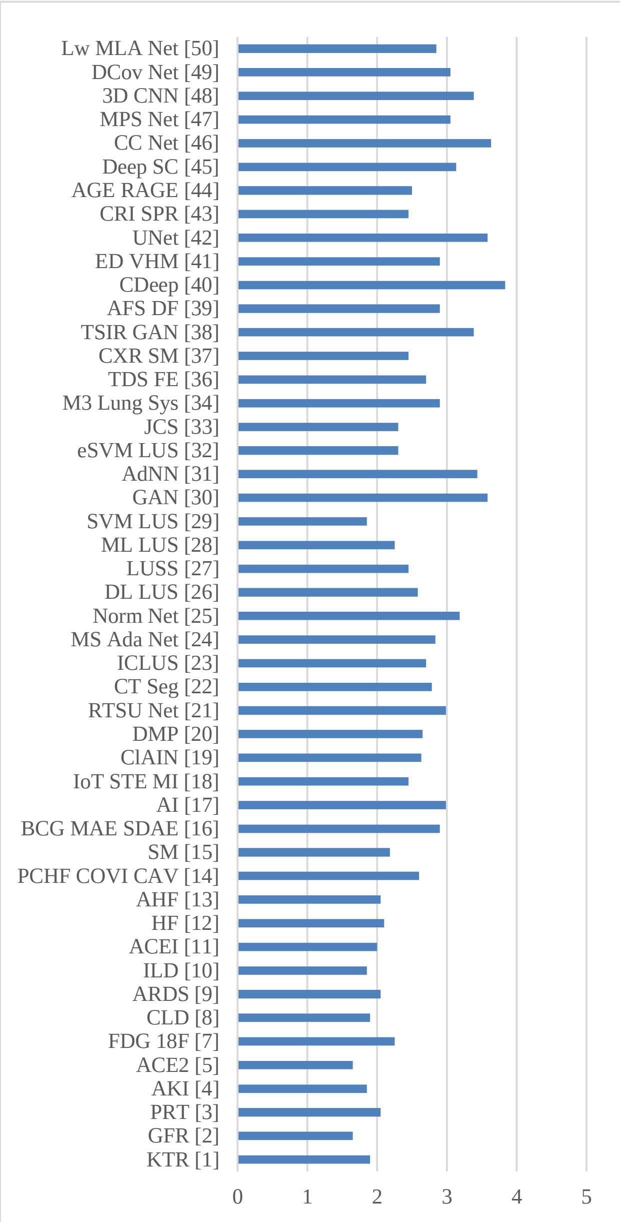

Figure 1. CCRM for different models

Based on this evaluation, it can be observed that Norm Net [25], GAN [30], AdNN [31], TSIR GAN [38], CDeep [40], UNet [42], Deep SC [45], MPS Net [47], 3D CNN [48], and DCov Net [49] showcase higher accuracy, while GAN [30], CDeep [40], UNet [42], CC Net [46], 3D CNN [48], and Lw MLA Net [50] showcase better precision, thus can be used for a wide variety of real-time clinical scenarios.

Similarly, AdNN [31], CDeep [40], SM [15], ClAIN [19], RTSU Net [21], MS Ada Net [24], UNet [42], Deep SC [45], and CC Net [46] have lower delay, while ClAIN [19], MS Ada Net [24], and CC Net [46] are able to achieve lower cost, which makes them useful for real-time and high-speed use cases.

While, in terms of scalability, GAN [30], TSIR GAN [38], CDeep [40], UNet [42], and CC Net [46] are useful for a wide variety of real-time clinical scenarios.

All these metrics were combined to form a novel CoVID19 Classification Rank Metric (CCRM), which is evaluated via equation 1, and combines these parameters for comprehensive identification of optimal models.

$$CCRM = \frac{A + P + S}{5} + \frac{1}{D} + \frac{1}{DC} \ldots (1)$$

Based on this evaluation and figure 1, it can be observed that CDeep [40], CC Net [46], GAN [30], UNet [42], AdNN [31], TSIR GAN [38], 3D CNN [48], Norm Net [25], Deep SC [45], MPS Net [47], and DCov Net [49] showcase better overall performance, thus can be used for multimodal analysis of different CoVID19 based side effects under clinical scenarios.

4. Conclusion & future scope

The comprehensive examination of previously developed CoVID19 analysis models reveals that these models exhibit a great deal of diversity in terms of the scope of problems they can solve and the quality of the results they provide. On the basis of their comparative investigation, it was found that Norm Net [25], GAN [30], AdNN [31], TSIR GAN [38], CDeep [40], UNet [42], Deep SC [45], MPS Net [47], 3D CNN [48], and DCov Net [49] exhibit higher accuracy, while GAN [30], CDeep [40], UNet [42], CC Net [46], and 3D CNN

[48] exhibit better precision, In a similar fashion, AdNN [31], CDeep [40], SM [15], ClAIN [19], RTSU Net [21], MS Ada Net [24], UNet [42], Deep SC [45], and CC Net [46] have a lower delay, and ClAIN [19], MS Ada Net [24], and CC Net [46] are able to achieve a lower cost, which enables them to be useful for real-time and high-speed use cases. While GAN [30], TSIR GAN [38], CDeep [40], UNet [42], and CC Net [46] are beneficial for a broad range of real-time clinical settings, these networks are not scalable. When these metrics were combined, it was discovered that CDeep [40], CC Net [46], GAN [30], UNet [42], AdNN [31], TSIR GAN [38], 3D CNN [48], Norm Net [25], Deep SC [45], MPS Net [47], and DCov Net [49] showcase better overall performance. As a result, these networks are capable of being used for multimodal analysis of various CoVID19-based side effects within clinical settings. In the future, researchers will need to test these models using a variety of clinical datasets and make advantage of their hybrid configurations in order to further increase overall performance levels. These models need to also be evaluated under various types of disease, and they can be extended by making use of bioinspired models, Autoencoders, Generative Adversarial Networks (GANs), Q-Learning techniques, and other such methods, all of which will help in incrementally improving their real-time performance levels for various types of disease in clinical scenarios.

5. Conflict of Interest

There is no conflict of interest. The authors declares the same.

6. References

[1] Kute, VB, Meshram, HS, Navadiya, VV, et al. Consequences of the first and second C-19 wave on kidney transplant recipients at a large Indian transplant centre. *Nephrology*. 2022; 27(2): 195- 207. doi:10.1111/nep.13961

[2] van Laar, SA, de Boer, MGJ, Gombert-Handoko, KB, Guchelaar, H-J, Zwaveling, J, . Liver and kidney function in patients with C-19 treated with remdesivir. *Br J Clin Pharmacol*. 2021; 87(11): 4450-4454. https://doi.org/10.1111/bcp.14831

[3] Han, X, Ye, Q. Kidney involvement in C-19 and its treatments. *J Med Virol*. 2021; 93: 1387–1395. https://doi.org/10.1002/jmv.26653

[4] Goh, BL, Shanmuganathan, M, Peariasamy, K, et al. C-19 death and kidney disease in a multiracial Asian country. *Nephrology*. 2022; 27(7): 566- 576. doi:10.1111/nep.14045

[5] Ahmadian, E., Hosseiniyan Khatibi, S.M., Razi Soofiyani, S., Abediazar, S., Shoja, M.M., Ardalan, M. and Zununi Vahed, S. (2021), C-19 and kidney injury: Pathophysiology and molecular mechanisms. Rev Med Virol, 31: e2176. https://doi.org/10.1002/rmv.2176

[6] Waldrop, G., Safavynia, S.A., Barra, M.E., Agarwal, S., Berlin, D.A., Boehme, A.K., Brodie, D., Choi, J.M., Doyle, K., Fins, J.J., Ganglberger, W., Hoffman, K., Mittel, A.M., Roh, D., Mukerji, S.S., Der Nigoghossian, C., Park, S., Schenck, E.J., Salazar-Schicchi, J., Shen, Q., Sholle, E., Velazquez, A.G., Walline, M.C., Westover, M.B., Brown, E.N., Victor, J., Edlow, B.L., Schiff, N.D. and Claassen, J. (2022), Prolonged Unconsciousness is Common in C-19 and Associated with Hypoxemia. Ann Neurol, 91: 740-755. https://doi.org/10.1002/ana.26342

[7] Guedj, E., Campion, J.-Y., Horowitz, T., Barthelemy, F., Cammilleri, S., & Ceccaldi, M. (2022). The impact of C-19 lockdown on brain metabolism. *Human Brain Mapping*, 43(2), 593–597. https://doi.org/10.1002/hbm.25673

[8] Martinez, M.A. and Franco, S. (2021), Impact of C-19 in Liver Disease Progression. Hepatol Commun, 5: 1138-1150. https://doi.org/10.1002/hep4.1745

[9] Nardo, AD, Schneeweiss-Gleixner, M, Bakail, M, Dixon, ED, Lax, SF, Trauner, M. Pathophysiological mechanisms of liver injury in C-19. *Liver Int*. 2021; 41: 20–32. https://doi.org/10.1111/liv.14730

[10] Schaefer, E.A.K., Arvind, A., Bloom, P.P. and Chung, R.T. (2020), Interrelationship Between Coronavirus Infection and Liver Disease. Clinical Liver Disease, 15: 175-180. https://doi.org/10.1002/cld.967

[11] Morishita, T., Takada, D., Shin, J., Higuchi, T., Kunisawa, S., Fushimi, K., and Imanaka, Y. (2022) Effects of the C-19 pandemic on heart failure hospitalizations in Japan: interrupted time series analysis. *ESC Heart Failure*, 9: 31–38. https://doi.org/10.1002/ehf2.13744.

[12] Chatrath, N., Kaza, N., Pabari, P. A., Fox, K., Mayet, J., Barton, C., Cole, G. D.,

and Plymen, C. M. (2020) The effect of concomitant C-19 infection on outcomes in patients hospitalized with heart failure. *ESC Heart Failure*, 7: 4443–4447. https://doi.org/10.1002/ehf2.13059.

[13] Kubica, J., Ostrowska, M., Stolarek, W., Kasprzak, M., Grzelakowska, K., Kryś, J., Kubica, A., Adamski, P., Podhajski, P., Navarese, E. P., Anielska-Michalak, E., Brycht, O., Curzytek, A., Dudek, A., Gromadziński, L., Grzelakowski, P., Kamiński, L., Kleinrok, A., Kostkiewicz, M., Koziński, M., Król, P., Kulawik, T., Minczew, G., Mindykowski, M., Pawlak, A., Prokopczuk, J., Skonieczny, G., Sobkowicz, B., Sowiński, S., Stankala, S., Szymański, P., Wester, A., Wilczewski, P., Bartuś, S., Budaj, A., Gąsior, M., Gruchała, M., Drożdż, J., Jaguszewski, M., Jankowski, P., Legutko, J., Lesiak, M., Leszek, P., Mitkowski, P., Nessler, J., Tomaszuk-Kazberuk, A., Tycińska, A., Zdrojewski, T., and Kaźmierczak, J. (2022) Impact of C-19 pandemic on acute heart failure admissions and mortality: a multicentre study (COV-HF-SIRIO 6 study). *ESC Heart Failure*, 9: 721–728. https://doi.org/10.1002/ehf2.13680.

[14] Sokolski, M., Trenson, S., Sokolska, J. M., D'Amario, D., Meyer, P., Poku, N. K., Biering-Sørensen, T., Højbjerg Lassen, M. C., Skaarup, K. G., Barge-Caballero, E., Pouleur, A.-C., Stolfo, D., Sinagra, G., Ablasser, K., Muster, V., Rainer, P. P., Wallner, M., Chiodini, A., Heiniger, P. S., Mikulicic, F., Schwaiger, J., Winnik, S., Cakmak, H. A., Gaudenzi, M., Mapelli, M., Mattavelli, I., Paul, M., Cabac-Pogorevici, I., Bouleti, C., Lilliu, M., Minoia, C., Dauw, J., Costa, J., Celik, A., Mewton, N., Montenegro, C. E. L., Matsue, Y., Loncar, G., Marchel, M., Bechlioulis, A., Michalis, L., Dörr, M., Prihadi, E., Schoenrath, F., Messroghli, D. R., Mullens, W., Lund, L. H., Rosano, G. M. C., Ponikowski, P., Ruschitzka, F., and Flammer, A. J. (2021) Heart failure in C-19: the multicentre, multinational PCHF-COVICAV registry. *ESC Heart Failure*, 8: 4955–4967. https://doi.org/10.1002/ehf2.13549.

[15] T. F. Quatieri, T. Talkar and J. S. Palmer, "A Framework for Biomarkers of C-19 Based on Coordination of Speech-Production Subsystems," in IEEE Open Journal of Engineering in Medicine and Biology, vol. 1, pp. 203-206, 2020, doi: 10.1109/OJEMB.2020.2998051.

[16] J. Liu, F. Miao, L. Yin, Z. Pang and Y. Li, "A Noncontact Ballistocardiography-Based IoMT System for Cardiopulmonary Health Monitoring of Discharged C-19 Patients," in IEEE Internet of Things Journal, vol. 8, no. 21, pp. 15807-15817, 1 Nov.1, 2021, doi: 10.1109/JIOT.2021.3063549.

[17] W. Jiang et al., "A Wearable Tele-Health System towards Monitoring C-19 and Chronic Diseases," in IEEE Reviews in Biomedical Engineering, vol. 15, pp. 61-84, 2022, doi: 10.1109/RBME.2021.3069815.

[18] N. Ji et al., "Recommendation to Use Wearable-Based mHealth in Closed-Loop Management of Acute Cardiovascular Disease Patients During the C-19 Pandemic," in IEEE Journal of Biomedical and Health Informatics, vol. 25, no. 4, pp. 903-908, April 2021, doi: 10.1109/JBHI.2021.3059883.

[19] N. Ji et al., "Recommendation to Use Wearable-Based mHealth in Closed-Loop Management of Acute Cardiovascular Disease Patients During the C-19 Pandemic," in IEEE Journal of Biomedical and Health Informatics, vol. 25, no. 4, pp. 903-908, April 2021, doi: 10.1109/JBHI.2021.3059883.

[20] H. R. Hasan et al., "Blockchain-Based Solution for C-19 Digital Medical Passports and Immunity Certificates," in IEEE Access, vol. 8, pp. 222093-222108, 2020, doi: 10.1109/ACCESS.2020.3043350.

[21] W. Xie, C. Jacobs, J. -P. Charbonnier and B. van Ginneken, "Relational Modeling for Robust and Efficient Pulmonary Lobe Segmentation in CT Scans," in IEEE Transactions on Medical Imaging, vol. 39, no. 8, pp. 2664-2675, Aug. 2020, doi: 10.1109/TMI.2020.2995108.

[22] Y. Zhang, Q. Liao, L. Yuan, H. Zhu, J. Xing and J. Zhang, "Exploiting Shared Knowledge From Non-COVID Lesions for Annotation-Efficient C-19 CT Lung Infection Segmentation," in IEEE Journal of Biomedical and Health Informatics, vol. 25, no. 11, pp. 4152-4162, Nov. 2021, doi: 10.1109/JBHI.2021.3106341.

[23] O. Frank et al., "Integrating Domain Knowledge Into Deep Networks for Lung Ultrasound With Applications to C-19," in IEEE Transactions on Medical Imaging, vol.

41, no. 3, pp. 571-581, March 2022, doi: 10.1109/TMI.2021.3117246.

[24] J. An, Q. Cai, Z. Qu and Z. Gao, "C-19 Screening in Chest X-Ray Images Using Lung Region Priors," in IEEE Journal of Biomedical and Health Informatics, vol. 25, no. 11, pp. 4119-4127, Nov. 2021, doi: 10.1109/JBHI.2021.3104629.

[25] Q. Yao, L. Xiao, P. Liu and S. K. Zhou, "Label-Free Segmentation of C-19 Lesions in Lung CT," in IEEE Transactions on Medical Imaging, vol. 40, no. 10, pp. 2808-2819, Oct. 2021, doi: 10.1109/TMI.2021.3066161.

[26] U. Khan et al., "Deep Learning-Based Classification of Reduced Lung Ultrasound Data From C-19 Patients," in IEEE Transactions on Ultrasonics, Ferroelectrics, and Frequency Control, vol. 69, no. 5, pp. 1661-1669, May 2022, doi: 10.1109/TUFFC.2022.3161716.

[27] J. Chen et al., "Quantitative Analysis and Automated Lung Ultrasound Scoring for Evaluating C-19 Pneumonia With Neural Networks," in IEEE Transactions on Ultrasonics, Ferroelectrics, and Frequency Control, vol. 68, no. 7, pp. 2507-2515, July 2021, doi: 10.1109/TUFFC.2021.3070696.

[28] S. Roy et al., "Deep Learning for Classification and Localization of C-19 Markers in Point-of-Care Lung Ultrasound," in IEEE Transactions on Medical Imaging, vol. 39, no. 8, pp. 2676-2687, Aug. 2020, doi: 10.1109/TMI.2020.2994459.

[29] L. Carrer et al., "Automatic Pleural Line Extraction and C-19 Scoring From Lung Ultrasound Data," in IEEE Transactions on Ultrasonics, Ferroelectrics, and Frequency Control, vol. 67, no. 11, pp. 2207-2217, Nov. 2020, doi: 10.1109/TUFFC.2020.3005512.

[30] Z. Yang, L. Zhao, S. Wu and C. Y. -C. Chen, "Lung Lesion Localization of C-19 From Chest CT Image: A Novel Weakly Supervised Learning Method," in IEEE Journal of Biomedical and Health Informatics, vol. 25, no. 6, pp. 1864-1872, June 2021, doi: 10.1109/JBHI.2021.3067465.

[31] R. Wang, C. Ji, Y. Zhang and Y. Li, "Focus, Fusion, and Rectify: Context-Aware Learning for C-19 Lung Infection Segmentation," in IEEE Transactions on Neural Networks and Learning Systems, vol. 33, no. 1, pp. 12-24, Jan. 2022, doi: 10.1109/TNNLS.2021.3126305.

[32] Y. Wang, Y. Zhang, Q. He, H. Liao and J. Luo, "Quantitative Analysis of Pleural Line and B-Lines in Lung Ultrasound Images for Severity Assessment of C-19 Pneumonia," in IEEE Transactions on Ultrasonics, Ferroelectrics, and Frequency Control, vol. 69, no. 1, pp. 73-83, Jan. 2022, doi: 10.1109/TUFFC.2021.3107598.

[33] Y. -H. Wu et al., "JCS: An Explainable C-19 Diagnosis System by Joint Classification and Segmentation," in IEEE Transactions on Image Processing, vol. 30, pp. 3113-3126, 2021, doi: 10.1109/TIP.2021.3058783.

[34] X. Qian et al., "M^{3}Lung-Sys: A Deep Learning System for Multi-Class Lung Pneumonia Screening From CT Imaging," in IEEE Journal of Biomedical and Health Informatics, vol. 24, no. 12, pp. 3539-3550, Dec. 2020, doi: 10.1109/JBHI.2020.3030853.

[35] G. Subramanian and A. Sreekantan Thampy, "Implementation of Blockchain Consortium to Prioritize Diabetes Patients' Healthcare in Pandemic Situations," in IEEE Access, vol. 9, pp. 162459-162475, 2021, doi: 10.1109/ACCESS.2021.3132302.

[36] Y. -H. Taguchi and T. Turki, "Application of Tensor Decomposition to Gene Expression of Infection of Mouse Hepatitis Virus Can Identify Critical Human Genes and Efffective Drugs for SARS-CoV-2 Infection," in IEEE Journal of Selected Topics in Signal Processing, vol. 15, no. 3, pp. 746-758, April 2021, doi: 10.1109/JSTSP.2021.3061251.

[37] Y. Oh, S. Park and J. C. Ye, "Deep Learning C-19 Features on CXR Using Limited Training Data Sets," in IEEE Transactions on Medical Imaging, vol. 39, no. 8, pp. 2688-2700, Aug. 2020, doi: 10.1109/TMI.2020.2993291.

[38] H. Wang et al., "Predicting the Epidemics Trend of C-19 Using Epidemiological-Based Generative Adversarial Networks," in IEEE Journal of Selected Topics in Signal Processing, vol. 16, no. 2, pp. 276-288, Feb. 2022, doi: 10.1109/JSTSP.2022.3152375.

[39] L. Sun et al., "Adaptive Feature Selection Guided Deep Forest for C-19 Classification With Chest CT," in IEEE Journal of Biomedical and Health Informatics, vol. 24, no. 10, pp. 2798-2805, Oct. 2020, doi: 10.1109/JBHI.2020.3019505.

[40] S. Hassantabar et al., "CovidDeep: SARS-CoV-2/C-19 Test Based on Wearable Medical Sensors and Efficient Neural Networks," in

IEEE Transactions on Consumer Electronics, vol. 67, no. 4, pp. 244-256, Nov. 2021, doi: 10.1109/TCE.2021.3130228.

[41] R. R. Sharma, M. Kumar, S. Maheshwari and K. P. Ray, "EVDHM-ARIMA-Based Time Series Forecasting Model and Its Application for C-19 Cases," in IEEE Transactions on Instrumentation and Measurement, vol. 70, pp. 1-10, 2021, Art no. 6502210, doi: 10.1109/TIM.2020.3041833.

[42] X. Wang et al., "A Weakly-Supervised Framework for C-19 Classification and Lesion Localization From Chest CT," in IEEE Transactions on Medical Imaging, vol. 39, no. 8, pp. 2615-2625, Aug. 2020, doi: 10.1109/TMI.2020.2995965.

[43] B. Gharizadeh et al., "Navigating the Pandemic Response Life Cycle: Molecular Diagnostics and Immunoassays in the Context of C-19 Management," in IEEE Reviews in Biomedical Engineering, vol. 14, pp. 30-47, 2021, doi: 10.1109/RBME.2020.2991444.

[44] B. Chakrabarty, D. Das, G. Bulusu and A. Roy, "Network-Based Analysis of Fatal Comorbidities of C-19 and Potential Therapeutics," in IEEE/ACM Transactions on Computational Biology and Bioinformatics, vol. 18, no. 4, pp. 1271-1280, 1 July-Aug. 2021, doi: 10.1109/TCBB.2021.3075299.

[45] X. Wang et al., "Joint Learning of 3D Lesion Segmentation and Classification for Explainable C-19 Diagnosis," in IEEE Transactions on Medical Imaging, vol. 40, no. 9, pp. 2463-2476, Sept. 2021, doi: 10.1109/TMI.2021.3079709.

[46] F. Li, X. Lu and J. Yuan, "MHA-CoroCapsule: Multi-Head Attention Routing-Based Capsule Network for C-19 Chest X-Ray Image Classification," in IEEE Transactions on Medical Imaging, vol. 41, no. 5, pp. 1208-1218, May 2022, doi: 10.1109/TMI.2021.3134270.

[47] H. -Y. Pei, D. Yang, G. -R. Liu and T. Lu, "MPS-Net: Multi-Point Supervised Network for CT Image Segmentation of C-19," in IEEE Access, vol. 9, pp. 47144-47153, 2021, doi: 10.1109/ACCESS.2021.3067047.

[48] X. Ouyang et al., "Dual-Sampling Attention Network for Diagnosis of C-19 From Community Acquired Pneumonia," in IEEE Transactions on Medical Imaging, vol. 39, no. 8, pp. 2595-2605, Aug. 2020, doi: 10.1109/TMI.2020.2995508.

[49] D. Singh, V. Kumar, M. Kaur, M. Y. Jabarulla and H. -N. Lee, "Screening of C-19 Suspected Subjects Using Multi-Crossover Genetic Algorithm Based Dense Convolutional Neural Network," in IEEE Access, vol. 9, pp. 142566-142580, 2021, doi: 10.1109/ACCESS.2021.3120717.

[50] K. Roy, D. Banik, D. Bhattacharjee, O. Krejcar and C. Kollmann, "LwMLA-NET: A Lightweight Multi-Level Attention-Based NETwork for Segmentation of C-19 Lungs Abnormalities From CT Images," in IEEE Transactions on Instrumentation and Measurement, vol. 71, pp. 1-13, 2022, Art no. 5007813, doi: 10.1109/TIM.2022.3161690.